Robotica (2005) volume 23, pp. 21–33. © 2005 Cambridge University Press
DOI: 10.1017/S026357470400058X Printed in the United Kingdom

Open-loop stable running

Katja D. Mombaur*, Richard W. Longman†, Hans Georg Bock* and Johannes P. Schlöder*

(Received in Final Form: May 21, 2004)

SUMMARY
We present simulated monopedal and bipedal robots that are capable of open-loop stable periodic running motions without any feedback even though they have no statically stable standing positions. Running as opposed to walking involves flight phases which makes stability a particularly difficult issue. The concept of open-loop stability implies that the actuators receive purely periodic torque or force inputs that are never altered by any feedback in order to prevent the robot from falling. The design of these robots and the choice of model parameter values leading to stable motions is a difficult task that has been accomplished using newly developed stability optimization methods.

KEYWORDS: Running robots; Monopod; Biped; Open-loop stable motions; Stability optimization

1. INTRODUCTION

In this paper, we investigate periodic running motions of one- and two-legged robots. By definition, running motions involve flight phases, in contrast to walking motions where always at least one foot is in contact with the ground. For monopod robots, running (also termed hopping in this case) is obviously the only possible form of locomotion. Due to the increased speed of motion, running robots are much harder to operate than walking robots: On the one hand, they need more powerful motors which however should not be too heavy and, on the other hand, the stability control task becomes much harder since the response times get smaller. Our work focuses on the stability aspect of running.

The classical control concept for walking and running robots is feedback control. A real-time closed-loop control of these walking robots requires sophisticated and expensive sensory systems and feedback-controllers. The computation of appropriate feedback is time critical and often a limitation for making motions faster, hence demanding for high computational capacities on-board. This all translates into the necessity of high budgets and deep technical knowledge.

Our approach to the stability control issue is to determine, in a first step, what can be achieved without any active feedback, and to search in fact for purely open-loop controlled, self-stabilizing system configurations and running motions. This implies

- that there is no feedback and no sensors at all, not even a detection of contact times
- that the robots response is only based on its natural dynamics, i.e. its inherent kinematic in kinetic properties
- that the system input (i.e. the joint torques etc.) which is continuously active over the full cycle and not impulse-like is never modified (not even the actuation cycle frequency)
- that the robot motion must always stay synchronized with the invariable external exciting frequency and that there is no possibility of time shifts.

These rules may seem very strict, since some types of feedback (like a phase adjustment at contact events) are easily implementable, but we consider these purely open-loop stable solutions to be good starting points for an experimental phase in which the robots motion can then be made more robust by simple feedback measures.

Running and hopping motions of one-legged robots have been investigated by a number of authors in theory and experiment, mainly implementing simple feedback control laws. Raibert & Sutherland[1] designed and manufactured a one-legged hopping robot consisting of a body and a springy leg. Monopods have also been built with an articulated instead of a springy leg, like OLIE of de Man et al.,[2] Vermeulen et al.[3] Running bipeds in 2D and 3D have been built and operated at MIT Leg Lab by Hodgins and Playter, respectively.[4]

In the field of passive dynamic robots, i.e. robots that have neither actuators nor active feedback, but are purely mechanical devices moving down inclined slopes, McGeer[6] investigated bipedal running and found stable solutions for some sets of parameters. The passive simulated point foot hopping robot of Thomson & Raibert[5] has only springs but – as the authors point out themselves – its motion is not stable.

Not much research has been done in the field of actuated open-loop stable running motions. Ringrose[7] was the first to discover that one-legged hopping is also possible without active feedback. However, this robot (as well as the more recent robot of Wei et al.[8]) relies on a very large circular foot, placing the center of the foot radius above or at least close to the center of mass. Cham et al.[9] detected self-stabilizing behavior in the motion of cockroaches. Buehler[10] investigated one-legged hopping robots (besides multi-legged walking robots) that are partly open-loop controlled, but also rely on some feedback concepts.

* IWR, Universität Heidelberg, Im Neuenheimer Feld 368, 69120 Heidelberg (Germany).
† Dept. of Mechanical Engineering, Columbia University, New York, 10027 (USA).
Corresponding author: K. D. Mombaur. Katja.Mombaur@IWR.Uni-Heidelberg.de

https://doi.org/10.1017/S026357470400058X Published online by Cambridge University Press

To our knowledge, the robots presented in this paper are the first actuated one- and two-legged running robots that are capable of self-stabilizing motions without any feedback while having only point feet. The self-stabilizing effects exploited by our robots are too complex to be explained in an intuitive manner. This also implies that finding these stable configurations is a difficult task that cannot be solved intuitively. Determining model parameter values that allow a stable periodic hopping motion was only possible by means of numerical stability optimization methods that we developed specifically for this purpose. Stability is defined in terms of the spectral radius of the monodromy matrix. This criterion has been applied to gaits before by various authors (e.g. McGeer,[11] Coleman,[12] Cheng & Lin,[13] Hurmuzlu[14]), but only to analyze the stability of a given gait cycle. In contrast to this approach, we use this stability definition as an optimization criterion in the design phase of the gait system. This objective function is non-differentiable, it may be non-Lipschitz at points of multiple maximum eigenvalue, and it involves the derivatives of the Poincaré mapping, thus representing a difficult non-standard optimization criterion. We introduce a two-level stability optimization procedure splitting the problems of periodic gait generation and stabilization of the system. We use a combination of efficient state-of the art gradient based optimization methods and direct search methods to cope with the difficulties of this problem. The same stability optimization method has previously been used to determine e.g. open-loop stable human-like walking (Mombaur et al.[15]). The methods presented in this paper are taken from the recent thesis of Mombaur.[16]

The remainder of this paper is organized as follows: The one- and two-legged running models investigated in this paper are described in section 2 including the full set of model equations. The stability optimization methods are described in section 3. In sections 4 and 5, we finally present the most stable solution found with these methods for point foot running robots with one and two legs, respectively.

2. MATHEMATICAL MODELS OF RUNNING

Periodic motions of running and walking robots are described by complex nonlinear systems of differential equations with multiple phases, discontinuities at implicitly defined switching points, and complex nonlinear constraints. In this paper, two different models of running will be considered: a running (or hopping) monopod and a running biped which both perform planar motions on level ground with alternating flight and single-foot contact phases. In this section, we give the full sets of equations for both robot models.

2.1. Model of one-legged hopping robot

The one-legged hopping robot consists of a trunk and a single telescopic leg which is coupled to he trunk by an actuated hinge. The two parts of the leg are connected by an actuated spring-damper element. We also have investigated model versions with circular feet,[16] but we focus on the more interesting point foot version in the present paper. In all cases, the foot is fixed to the lower leg without articulation. The design of the robot and especially of the leg has been

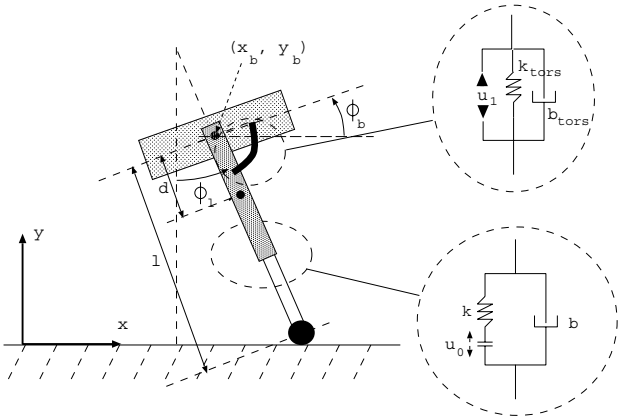

Fig. 1. Parameters, controls, and coordinates of one-legged hopping robot.

inspired by the simple monopod of Ringrose[7] but it is more complex since it has a separate upper body, and it is harder to stabilize due to the much smaller foot. The monopod can perform stable hopping motions including a non-sliding or rolling contact phase and a flight phase without any feedback controllers. In this paper we concentrate on the study of two-dimensional motions and their stability. The system is holonomic, but non-conservative due to damper forces and inelastic impacts. The latter property may promote stability of the system.

A sketch of the model and its parameters is given in figure 1. Model parameters are the robot's trunk mass and inertia m_b and Θ_b, leg mass and inertia m_l and Θ_l, distance between centers of mass of trunk and leg d, leg rest length l_0, torsional spring and damper constants k_{tors} and b_{tors}, rest location of torsional spring $\Delta\phi$, and translational spring and damper constants k and b. The foot is assumed to be massless.

During the flight phase, the robot has four degrees of freedom (DOF). As state variables we choose the uniform set of coordinates $q = (x_b, y_b, \phi_b, \phi_l)^T$, and the corresponding velocities $\dot{q}$, where x_b and y_b are two-dimensional position coordinates of the trunk center of mass, and ϕ_b and ϕ_l are the orientations of trunk and leg, respectively.

The coordinates of the center of mass of the leg, x_l and y_l, are eliminated using the distance parameter d by

$$x_l = x_b + d \sin\phi_l \tag{1}$$

$$y_l = y_b - d \cos\phi_l. \tag{2}$$

The leg length l is fixed to $l_0 + u_{SEA}$ during the major part of the flight phase (since the foot is massless) and depends on the other coordinates during the contact phase as follows:

$$l = \frac{y_b}{\cos\phi_l} \Rightarrow \tag{3}$$

$$\dot{l} = \frac{\dot{y}_b}{\cos\phi_l} + y_b \frac{\sin\phi_l}{\cos^2\phi_l}\dot{\phi}_l. \tag{4}$$

The robot has two actuators:

(i) u_{SEA} – series elastic actuator (SEA) in the prismatic joint: as described by Pratt et al.,[17] this is an actuated spring-damper element with spring constant k and damping

https://doi.org/10.1017/S026357470400058X Published online by Cambridge University Press

constant b (see figure 1). The control $u_{SEA} \geq 0$ actively changes the spring's length which has the same effect as changing the spring's rest length in the opposite direction:

$$\Delta l = \frac{y_b}{\cos\phi_l} - u_{SEA} - l_0 \tag{5}$$

The control u_{SEA} is only effective during the contact phase – due to the massless foot it can be brought back to zero position during flight without any effect. u_{SEA} is equal to zero at touchdown and has to be greater than zero at liftoff to compensate for the energy loss in the damper. Instantaneous compressions and general control histories can be modeled by our approach.

(ii) u_{tors} – torque control between trunk and leg (in parallel with a spring-damper-element k_{tors}, b_{tors}, see figure 1).

The equations of motion during the flight phase are described by the following set of ODEs:

$$\begin{pmatrix} m & 0 & 0 & m_l d\cos\phi_l \\ 0 & m & 0 & m_l d\sin\phi_l \\ 0 & 0 & \theta_b & 0 \\ -m_b d\cos\phi_l & -m_b d\sin\phi_l & & \theta_l \end{pmatrix} \cdot \begin{pmatrix} \ddot{x}_b \\ \ddot{y}_b \\ \ddot{\phi}_b \\ \ddot{\phi}_l \end{pmatrix}$$

$$= \begin{pmatrix} m_l d\sin\phi_l\dot{\phi}_l^2 \\ -m_l d\cos\phi_l\dot{\phi}_l^2 - mg \\ u_{tors} - k_{tors}(\phi_b - \phi_l - \Delta\phi) - b_{tors}(\dot{\phi}_b - \dot{\phi}_l) + m_b g d\sin\phi_l \\ -u_{tors} + m_b g d\sin\phi_l + k_{tors}(\phi_b - \phi_l - \Delta\phi) + b_{tors}(\dot{\phi}_b - \dot{\phi}_l) \end{pmatrix} \tag{6}$$

with u_{tors} being the torque between trunk and leg and $m = m_b + m_l$ the total mass.

During the contact phase the contact point is assumed to be fixed due to friction, but the leg length varies under the influence of the SEA spring-damper forces. This leads to a reduction from four to three DOF during contact phase which is described by the additional kinematic constraint in velocity space

$$\dot{x}_b + (y_b + y_b\tan^2\phi_l)\,\dot{\phi}_l + \tan\phi_l\,\dot{y}_b = 0. \tag{7}$$

A corresponding equation for the differences in position space can be formulated. The equations of motion for the contact phase become

with spring and damper forces F_k and F_d

$$F_k = k\left(\frac{y_b}{\cos\phi_l} - l_0 - u_{SEA}\right) \tag{9}$$

$$F_d = b\left(\frac{\dot{y}_b}{\cos\phi_l} + y_b\frac{\tan\phi_l}{\cos\phi_l}\dot{\phi}_l\right). \tag{10}$$

Phase change from contact phase to flight pase (liftoff) takes place, when the spring length is equal to the (modified) rest length:

$$s_{liftoff} = l_0 + u_{SEA} - \frac{y_b}{\cos\phi_l} = 0 \tag{11}$$

and, at the same time, the trunk has a positive vertical speed:

$$c_{liftoff} = \dot{y}_b > 0. \tag{12}$$

Touchdown phase change occurs when the height of the prospective contact point on the foot is equal to zero

$$s_{touchdown} = y_b - l_0\cos\phi_l = 0. \tag{13}$$

The vertical speed of the this point must be negative at touchdown:

$$c_{touchdown} = \dot{y}_b + l_0\sin\phi_l\dot{\phi}_l < 0. \tag{14}$$

There may be a discontinuity in the velocities at touchdown because friction is assumed to be large enough to instantaneously set the velocity of the contact point to zero. The four velocities after the touchdown-discontinuity are determined by the following four conditions:

- superposition of rolling motion and spring-damper action:

$$\dot{x}_{contact} = \dot{x}_b + l_0\cos\phi_l\dot{\phi}_l + \dot{y}_b\tan\phi_l + y_b\dot{\phi}_l\tan^2\phi_l = 0, \tag{15}$$

$$\begin{pmatrix} m & 0 & 0 & m_l d\cos\phi_l & 1 \\ 0 & m & 0 & m_l d\sin\phi_l & \tan\phi_l \\ 0 & 0 & \theta_b & 0 & 0 \\ -m_b d\cos\phi_l & -m_b d\sin\phi_l & & \theta_l & y_b + (y_b - r)\tan^2\phi_l \\ 1 & \tan\phi_l & 0 & y_b + (y_b - r)\tan^2\phi_l & 0 \end{pmatrix} \cdot \begin{pmatrix} \ddot{x}_b \\ \ddot{y}_b \\ \ddot{\phi}_b \\ \ddot{\phi}_l \\ \lambda \end{pmatrix}$$

$$= \begin{pmatrix} m_l d\sin\phi_l\dot{\phi}_l^2 + (F_k + F_d)\sin\phi_l \\ -m_l d\cos\phi_l\dot{\phi}_l^2 - mg - (F_k + F_d)\cos\phi_l \\ u_{tors} - k_{tors}(\phi_b - \phi_l - \Delta\phi) - b_{tors}(\dot{\phi}_b - \dot{\phi}_l) + m_b g d\sin\phi_l \\ -u_{tors} + m_b g d\sin\phi_l + k_{tors}(\phi_b - \phi_l - \Delta\phi) + b_{tors}(\dot{\phi}_b - \dot{\phi}_l) + (F_k + F_d)\sin\phi_l \\ -2\cdot\cos^{-2}\phi_l\dot{\phi}_l(\dot{y}_b + y_b\tan\phi_l\dot{\phi}_l) \end{pmatrix} \tag{8}$$

https://doi.org/10.1017/S026357470400058X Published online by Cambridge University Press

- conservation of angular momentum of trunk about contact point:

$$H_{trunk,hip} = \Theta_b \dot{\phi}_b = const., \tag{16}$$

- conservation of angular momentum of full robot about prospective contact point

$$\begin{aligned} H_{robot,contact} = {} & \Theta_b \dot{\phi}_b - m_b(y_b - y_c)\dot{x}_b \\ & + m_b(x_b - x_c)\dot{y}_b + \Theta_l \dot{\phi}_l - m_l(y_l - y_c)\dot{x}_l \\ & + m_l(x_l - x_c)\dot{y}_l = const., \end{aligned} \tag{17}$$

with

$$x_c = x_b + l_0 \sin\phi_l \tag{18}$$

$$y_c = y_b - l_0 \cos\phi_l \tag{19}$$

- conservation of translational momentum in direction of leg (considering spring-damper-force)

$$m(\dot{x}_b \sin\phi_l - \dot{y}_b \cos\phi_l) - F_k - F_d = const. \tag{20}$$

There is no velocity discontinuity at liftoff and no discontinuities in the position variables at all for the one-legged hopper.

The variable x_b describes the forward motion of the robot and is non-periodic. All other state variables have to satisfy periodicity constraints ($q_{red}(T) = q_{red}(0)$ and $\dot{q}(T) = \dot{q}(0)$) where the period T is to be determined by the optimization.

2.2. *Model of two-legged running robot*

The running biped is an extension of the above monopod with a second identical leg. It is capable of stable two-dimensional running motions with alternating flight and non-sliding single-foot contact phases without any feedback support. Since the biped model is identical to the monopod (except for the duplicate leg) and has the same model parameters, we will not go through the full model description again but only highlight the differences (Fig. 2).

Along with the leg also the actuators are duplicated, such that there is one torque actuator between the trunk and each leg, and a series elastic actuator in each leg. The biped has on degree of freedom more than the monopod which results

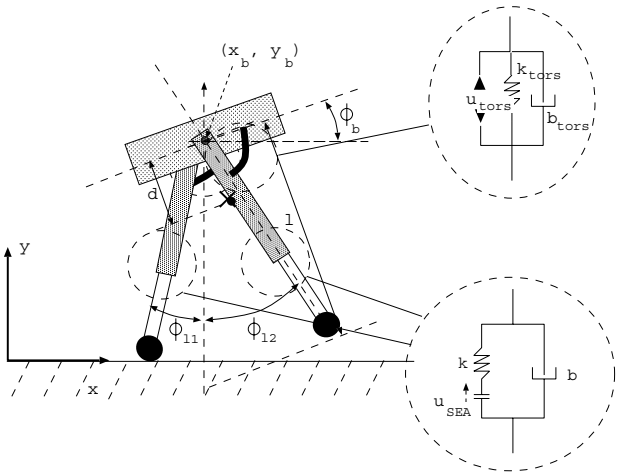

Fig. 2. Parameters, controls, and coordinates of two-legged running robot.

in five DOF during flight phase and four DOF during contact phase with the telescopic leg being unlocked. As state variables we choose the uniform set of coordinates

$$q = (x_b, y_b, \phi_b, \phi_{l,1}, \phi_{l,2})^T,$$

and the corresponding velocities, where x_b and y_b are the two-dimensional position coordinates of the trunk center of mass, and ϕ_b and $\phi_{l,1}$, $\phi_{l,2}$ are the orientations of the trunk and of the two legs. We do not model a full physical cycle which would consist of two steps but just one step (plus a leg shift to restore periodicity) since we are only interested in finding symmetric gait solutions. The cycle modeled starts right after touchdown with leg number one, goes through a full contact phase and a flight phase and ends right after touchdown with leg number two.

The motion during the flight phase is described by the following set of ODEs:

$$\begin{aligned} & \begin{pmatrix} m & 0 & 0 & m_l d\cos\phi_{l,1} & m_l d\cos\phi_{l,2} \\ 0 & m & 0 & m_l d\sin\phi_{l,1} & m_l d\sin\phi_{l,2} \\ 0 & 0 & \theta_b & 0 & 0 \\ m_l d\cos\phi_{l,1} & m_l d\sin\phi_{l,1} & 0 & \theta_l + m_l d^2 & 0 \\ m_l d\cos\phi_{l,2} & m_l d\sin\phi_{l,2} & 0 & 0 & \theta_l + m_l d^2 \end{pmatrix} \begin{pmatrix} \ddot{x}_b \\ \ddot{y}_b \\ \ddot{\phi}_b \\ \ddot{\phi}_{l,1} \\ \ddot{\phi}_{l,2} \end{pmatrix} \\ & = \begin{pmatrix} m_l d\left(\sin\phi_{l,1}\dot{\phi}_{l,1}^2 + \sin\phi_{l,2}\dot{\phi}_{l,2}^2\right) \\ -m_l d\left(\cos\phi_{l,1}\dot{\phi}_{l,1}^2 + \cos\phi_{l,2}\dot{\phi}_{l,2}^2\right) - mg \\ \sum_{i=1}^{2}(u_{tors,i} - k_{tors}(\phi_b - \phi_{l,i} - \Delta\phi) - b_{tors}(\dot{\phi}_b - \dot{\phi}_{l,i})) \\ -u_{tors,1} - m_l g d\sin\phi_{l,1} + k_{tors}(\phi_b - \phi_{l,1} - \Delta\phi) + b_{tors}(\dot{\phi}_b - \dot{\phi}_{l,1}) \\ -u_{tors,2} - m_l g d\sin\phi_{l,2} + k_{tors}(\phi_b - \phi_{l,2} - \Delta\phi) + b_{tors}(\dot{\phi}_b - \dot{\phi}_{l,2}) \end{pmatrix} \end{aligned} \tag{21}$$

where m is the total mass $m = m_b + 2m_l$ and $u_{tors,1}$ and $u_{tors,2}$ are the torques between trunk and leg one and two, respectively. The coupling of variables during the contact phase is described by the additional kinematic constraint in velocity space (contact with leg number one):

$$\dot{x}_b + (y_b + (y_b)\tan^2\phi_{l,1})\,\dot{\phi}_{l,1} + \tan\phi_{l,1}\,\dot{y}_b = 0 \tag{22}$$

https://doi.org/10.1017/S026357470400058X Published online by Cambridge University Press

and the equations of motion for the contact phase are described by the following DAE:

$$\begin{pmatrix} m & 0 & 0 & m_l d\cos\phi_{l,1} & m_l d\cos\phi_{l,2} & 1 \\ 0 & m & 0 & m_l d\sin\phi_{l,1} & m_l d\sin\phi_{l,2} & tan\phi_{l,1} \\ 0 & 0 & \theta_b & 0 & 0 & 0 \\ m_l d\cos\phi_{l,1} & m_l d\sin\phi_{l,1} & 0 & \theta_l + m_l d^2 & 0 & y_b(1+\tan^2\phi_{l,1}) \\ m_l d\cos\phi_{l,2} & m_l d\sin\phi_{l,2} & 0 & 0 & \theta_l + m_l d^2 & 0 \\ 1 & \tan\phi_{l,1} & 0 & y_b(1+\tan^2\phi_{l,1}) & 0 & 0 \end{pmatrix} \begin{pmatrix} \ddot{x}_b \\ \ddot{y}_b \\ \ddot{\phi}_b \\ \ddot{\phi}_{l,1} \\ \ddot{\phi}_{l,2} \\ \lambda \end{pmatrix}$$

$$= \begin{pmatrix} m_l d\left(\sin\phi_{l,1}\dot{\phi}_{l,1}^2 + \sin\phi_{l,2}\dot{\phi}_{l,2}^2\right) + (F_k + F_d)\sin\phi_{l,1} \\ -m_l d\left(\cos\phi_{l,1}\dot{\phi}_{l,1}^2 + \cos\phi_{l,2}\dot{\phi}_{l,2}^2\right) - mg - (F_k + F_d)\cos\phi_{l,1} \\ \sum_{i=1}^{2}(u_{tors,i} - k_{tors}(\phi_b - \phi_{l,i} - \Delta\phi) - b_{tors}(\dot{\phi}_b - \dot{\phi}_{l,i})) \\ -u_{tors,1} - m_l g d\sin\phi_{l,1} + k_{tors}(\phi_b - \phi_{l,1} - \Delta\phi) + b_{tors}(\dot{\phi}_b - \dot{\phi}_{l,1}) \\ -u_{tors,2} - m_l g d\sin\phi_{l,2} + k_{tors}(\phi_b - \phi_{l,2} - \Delta\phi) + b_{tors}(\dot{\phi}_b - \dot{\phi}_{l,2}) \\ -2\cdot\cos^{-2}\phi_{l,1}\dot{\phi}_{l,1}(\dot{y}_b + y_b\tan\phi_{l,1}\dot{\phi}_{l,1}) \end{pmatrix} \tag{23}$$

with spring and damper forces F_k and F_d

$$F_k = k\left(\frac{y_b}{\cos\phi_{l,1}} - l_0 - u_{SEA,1}\right) \tag{24}$$

$$F_d = b\left(\frac{\dot{y}_b}{\cos\phi_{l,1}} + y_b\frac{\tan\phi_{l,1}}{\cos\phi_{l,1}}\dot{\phi}_{l,1}\right) \tag{25}$$

Note that $u_{SEA,2}$ is not active during this step since leg number two has no ground contact.

Switching functions describing liftoff and touchdown for the running biped follow equations (11)–(14) for the monopod where ϕ_l and $\dot{\phi}_l$ need to be replaced by ϕ_{l_i} and $\dot{\phi}_{l_i}$ ($i = 1$ for liftoff and $i = 2$ for touchdown in this model).

The five velocities after the touchdown-discontinuity are determined by the following equations:

- non-sliding ground contact combined with spring-damper action:

$$\dot{x}_{contact} = \dot{x}_b + l_0\cos\phi_{l,2}\dot{\phi}_{l,2} + \dot{y}_b\tan\phi_{l,2} + y_b\dot{\phi}_{l,2}\tan^2\phi_{l,2} = 0 \tag{26}$$

- conservation of angular momentum of trunk about hip:

$$H_{trunk,hip} = \Theta_b\dot{\phi}_b = const. \tag{27}$$

- conservation of angular momentum of prospective swing leg (leg 1) about hip

$$H_{swingleg,hip} = (\Theta_l + m_l d^2)\dot{\phi}_{l,1} = const. \tag{28}$$

- conservation of angular momentum of full robot about prospective contact point

$$\begin{aligned} H_{robot,contact} = {} & \Theta_b\dot{\phi}_b - m_b(y_b - y_c)\dot{x}_b + m_b(x_b - x_c)\dot{y}_b \\ & + \Theta_{l,1}\dot{\phi}_{l,1} - m_l(y_{l,1} - y_c)\dot{x}_{l,1} \\ & + m_l(x_{l,1} - x_c)\dot{y}_{l,1} \\ & + \Theta_l\dot{\phi}_{l,2} - m_l(y_{l,2} - y_c)\dot{x}_{l,2} \\ & + m_l(x_{l,2} - x_c)\dot{y}_{l,2} = const. \end{aligned} \tag{29}$$

where $x_{l,i}$ and $y_{l,i}$ are determined by equations corresponding to (1) and (2) and with

$$x_c = x_b + l_0\sin\phi_{l,2} \tag{30}$$

$$y_c = y_b - l_0\cos\phi_{l,2} \tag{31}$$

- conservation of translational momentum in direction of prospective stance leg (considering spring-damper-force)

$$m(\dot{x}_b\sin\phi_l - \dot{y}_b\cos\phi_l) - F_k - F_d = const. \tag{32}$$

Again, there is no velocity discontinuity at liftoff. Positions are obviously continuous in a physical sense, however, since just one step is considered in the mathematical model, it also involves positions discontinuities due to the necessary switch of legs.

Periodicity constraints are applied to all position and velocity variables except for x_b which describes the forward motion.

3. OPTIMIZATION OF OPEN-LOOP STABILITY

In this section we sketch a numerical method for the optimization of open-loop stability of a periodic system that we developed recently. A detailed description of the method can be found in Mombaur[16] and Mombaur et al.[18] This is the first time stability optimization is combined with the simultaneous solution of a periodic optimal control problem. As shown in figure 3, we introduce a two-level approach splitting the problems of generating a periodic solution and of stabilizing this solution.

3.1. Outer Loop: Stabilization of a periodic gait

In the outer loop of the optimization procedure, model parameters are determined according to stability aspects. Stability is defined in terms of the spectral radius of the Jacobian C of the Poincaré map associated with the periodic solution.*

* This criterion describes the robustness of the periodic solution against small perturbations. Note that there are also completely different stability criteria for walking motions used by other authors (e.g. Garcia et al.,[19] Vukobratovic et al.[20]), but they are not suitable to chracterize the stability of a periodic bipedal or monopedal gait.

https://doi.org/10.1017/S026357470400058X Published online by Cambridge University Press

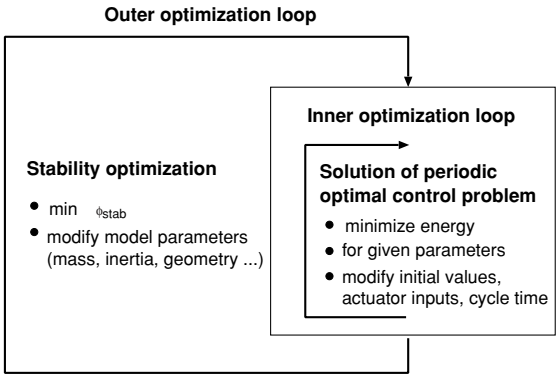

Fig. 3. Sketch of stability optimization procedure.

If the spectral radius is smaller than one, the solution is asymptotically stable, and if it is larger than one, the solution is unstable. We have proven that this criterion based on linear theory and typically applied to simple smooth systems can also be used to characterize the stability of solutions of a nonlinear multiphase system with discontinuities (Mombaur,[16] Mombaur et al.[18]). A similar proof has been given independently by Grizzle et al.[21] If the models include non-periodic variables, a projection of the monodromy matrix to the subspace of the periodic variables has to be performed to compute the correct Jacobian. We use the spectral radius as objective function of our optimization

$$\min_{p} |\lambda_{max}(C(p))|, \tag{33}$$

in the intention to decrease it below one.

The resulting optimization problem is difficult for two different reasons:

- The maximum eigenvalue function of the non-symmetric matrix C is non-differentiable and possibly even non-Lipschitz at points where multiple eigenvalues coalesce.
- The determination of the matrix C involves the computation of first order sensitivities of the discontinuous trajectories.

Any gradient-based optimization method would thus require second order derivatives of the trajectory which are extremely hard to compute, especially due to the discontinuities in the dynamics. For all reasons mentioned, a direct search method has proven to be a very good choice for the solution of this outer loop optimization problem. Direct search methods are optimization methods that solely use function information and do neither compute nor explicitely approximate derivatives. We have implemented a modification of the Nelder-Mead algorithm which is based on a polytope with $n+1$ vertices for optimization in n-dimensional space. According to the function information collected at its vertices the polytope expands in directions promising descent and contracts in bad directions. In contrast to the original method, we allow for multiple expansions in a promising direction, we use a different direction of contraction, and we only apply full polytope shrinking after multiple one-dimensional contractions. In addition, we consider the different nature of optimization variables by appropriate scaling of the initial polytope, we use a modified termination criterion, and we rely on a restart procedure as globalization strategy. Other than the original Nelder-Mead method, our algorithm can directly handle box constraints on the optimization variables not requiring a penalty function. For the type of problems described in this paper, the algorithm typically needs between 50 and several hundered steps to converge, where each step requires at least one solution (in the case of contractions and expansions several solutions) of the inner loop problem.

3.2. Inner loop: Generation of periodic gaits

The task of the inner loop is to find – for the set of parameters prescribed by the outer loop – actuator patterns, initial values and cycle time leading to a periodic trajectory. The choice of those variables is governed by energy consumption considerations (in terms of actuator inputs u). We also have imposed a lower bound on the trunk forward speed at all points, and bounds on the leg inclination angle at touchdown and liftoff instants. Together with the equations of motion, the periodicity constraints and phase switching conditions, box constraints on all variables etc. this leads to a multi-phase optimal control problem of the following form:

$$\min_{x,u,T} \int_0^T \|u\|_2^2 dt \tag{34}$$

$$\text{s. t.} \qquad \dot{x}(t) = f_j(t, x(t), u(t), p) \quad \text{or DAE} \tag{35}$$

$$x(\tau_j^+) = h(x(\tau_j^-)) \tag{36}$$

$$g_j(t, x(t), u(t), p) \geq 0 \tag{37}$$

$$\text{for} \quad t \in [\tau_{j-1}, \tau_j],$$

$$j = 1, \ldots, n_{ph},\ \tau_0 = 0, \tau_{n_{ph}} = T$$

$$r_{eq}(x(0), \ldots, x(T), p) = 0 \tag{38}$$

$$r_{ineq}(x(0), \ldots, x(T), p) \geq 0. \tag{39}$$

We solve this problem using a variant of the optimal control code MUSCOD (Bock & Plitt,[22] Leineweber[23]) suited for periodic gait problems. It is based on

- a direct method for the optimal control problem discretization using in this case a piecewise constant control discretization
- and a multiple shooting state parameterization which transforms the original boundary value problem into a set of initial value problems with corresponding continuity and boundary conditions.

When choosing identical grids for both discretization steps, one obtains a large but very structured non-linear programming problem. The solution of the discretized problem finally rests on two pillars:

- an efficient tailored SQP algorithm exploiting the structure of the problem (also compare Leineweber[24]).

https://doi.org/10.1017/S026357470400058X Published online by Cambridge University Press

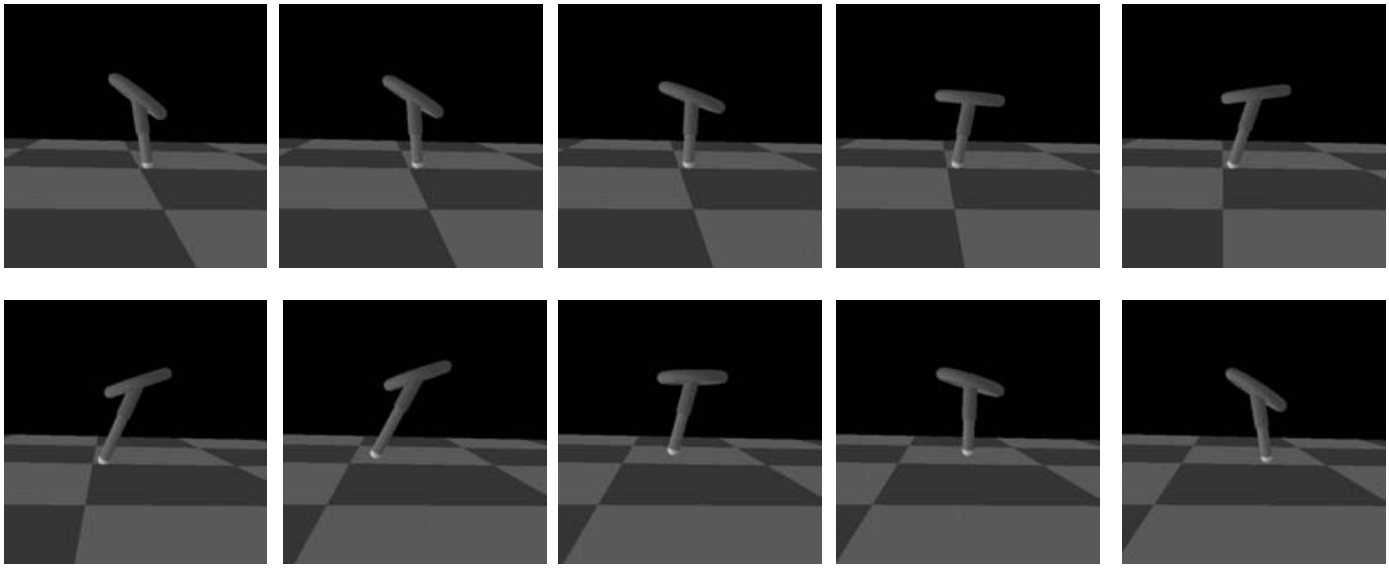

Fig. 4. Most stable open-loop controlled hopping motion.

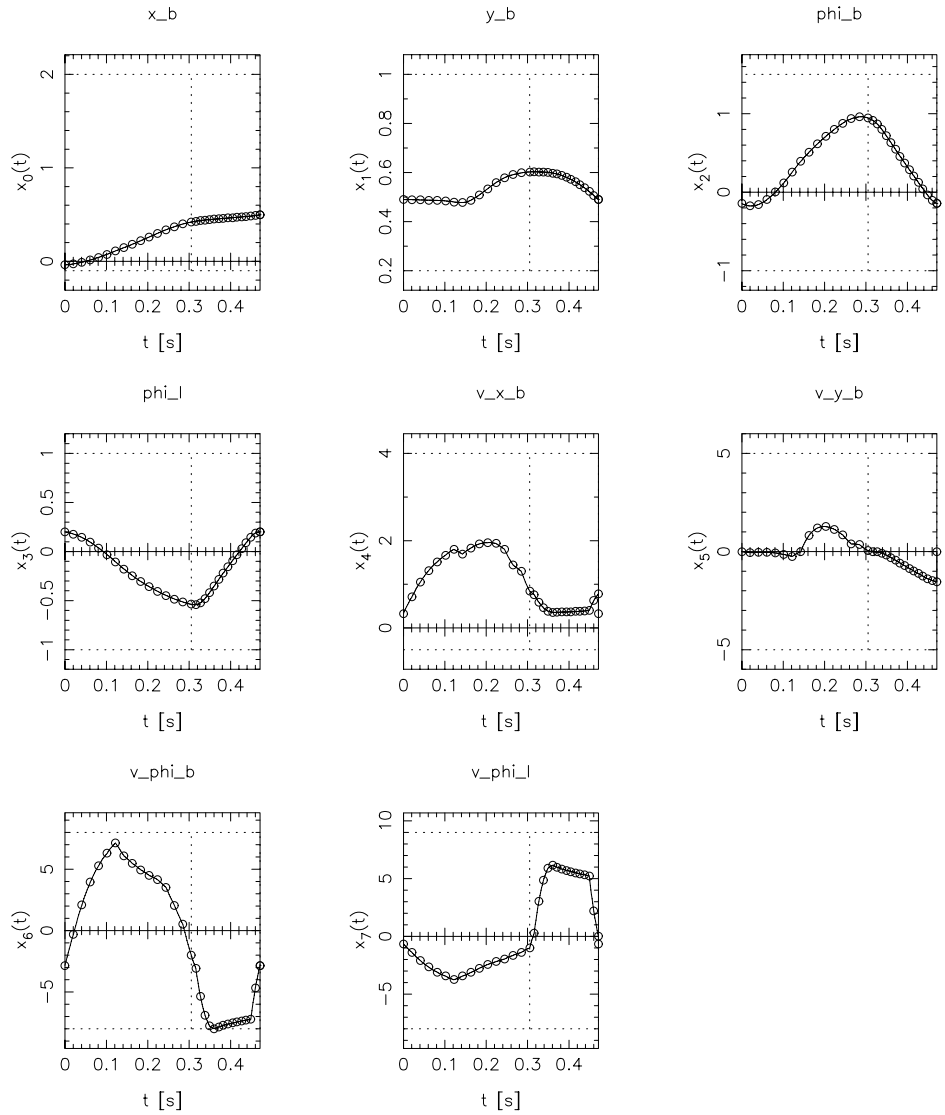

Fig. 5. Position and velocity trajectories of most stable solution of hopping robot.

https://doi.org/10.1017/S026357470400058X Published online by Cambridge University Press

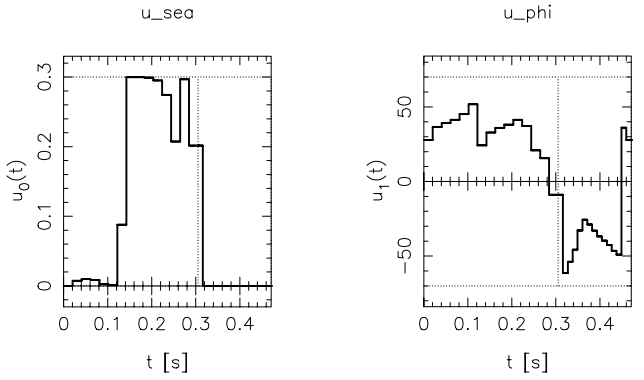

Fig. 6. Actuator inputs leading to most stable open-loop controlled solution of hopping robot.

- fast and reliable integration of the trajectories on the multiple shooting intervals including a computation of sensitivity information (Bock[24]).

Thanks to these efficient methods, the solution of a periodic optimal control problem for one of the robots treated in this paper only takes between a couple of seconds and half a minute (depending on the number of SQP steps) on a modern PC.

4. MOST STABLE SOLUTION OF THE ONE-LEGGED HOPPING ROBOT

In this section we present the most stable solution for the one-legged hopping robot that we found using the stability optimization methods described in the previous sections. We also have found stable solutions for robots with circular feet (but however with foot radii so small that the system is statically unstable) which are not presented here due to space limitations, and we refer to Mombaur[16] for further results.

The spectral radius of the most stable point foot solution is only 0.1292, i.e. far below one. A visualization of this solution with the Open GL-based tool JAFV by Winckler[25] is given in figure 4. Figure 5 shows plots of all position and velocity variables during one step of this periodic gait.

The model parameters of this solution are (in ISO units) $m_b = 2.0$, $\Theta_b = 0.3503$, $m_l = 0.5033$, $\Theta_l = 0.2391$, $d = 0.3663$, $l_0 = 0.5$, $r = 0$, $k_{tors} = 25.902$, $\Delta\phi_l = 0.2$, $b_{tors} = 3.457$, $k = 589.1$, and $b = 61.79$.

The initial values of the corresponding trajectory are

$$\begin{aligned} x_b(t_0) &= 0.0 & \dot{x}_b(t_0) &= 0.3326 \\ y_b(t_0) &= 0.49 & \dot{y}_b(t_0) &= 0.0011 \\ \phi_b(t_0) &= -0.1447 & \dot{\phi}_b(t_0) &= -2.8399 \\ \phi_l(t_0) &= 0.2 & \dot{\phi}_l(t_0) &= -0.6524. \end{aligned}$$

Since $x_b(0)$ is fixed to zero, $x_b(T)$ gives the step length of one hopping cycle, in this case 0.536 m. The cycle time of this solution is $T = 0.471$ s with phase times $T_{contact} = 0.305$ s and $T_{flight} = 0.166$ s. Figure 6 shows the periodic actuator histories for this most stable solution.

Due to the non-periodicity of x_b, only seven out of eight eigenvalues are relevant for stability. This last eigenvalue, which is always one because of the system's indifference towards the initial value $x_b(0)$, is eliminated by projection. The seven relevant eigenvalues are by magnitude

$$\begin{aligned} |\lambda_{1,2}| &= 0.1292 & |\lambda_5| &= 0.072172 \\ |\lambda_{3,4}| &= 0.1274 & |\lambda_{6,7}| &= 0 \end{aligned}$$

where the first two pairs are conjugate complex couples. The two eigenvalues of zero magnitude are caused by the reduction from four to three DOF during the contact phase

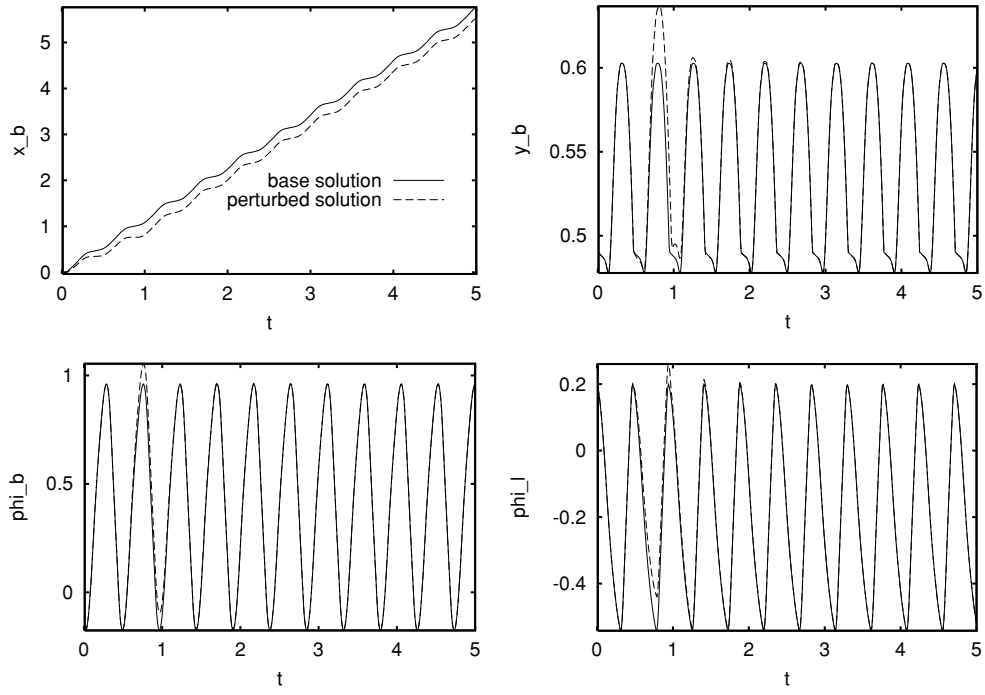

Fig. 7. Effect of perturbation (of $\dot{x}_b$ by -90%) on most stable trajectory of hopping robot.

https://doi.org/10.1017/S026357470400058X Published online by Cambridge University Press

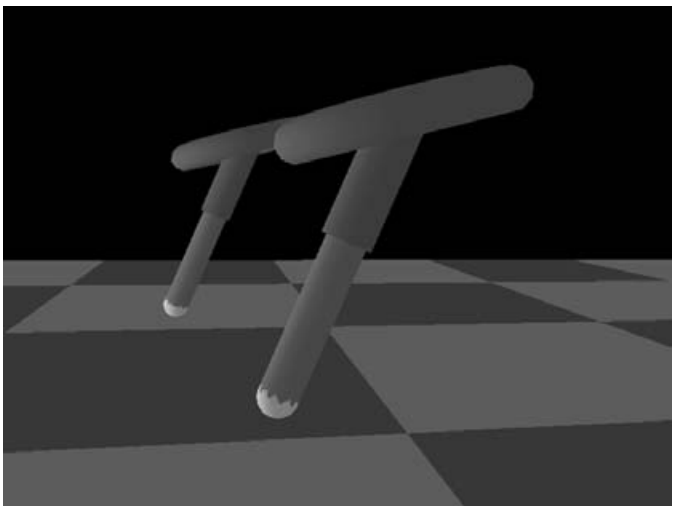

Fig. 8. Perturbed robot (back) stays behind unperturbed robot (front).

and the resulting coupling of perturbations in velocity as well as position space.

The size of the spectral radius does not say anything about the size of perturbations from which the system can recover, but they are particularly interesting for the practical use of the computational solution. We determine these stability margins numerically by applying one-dimensional perturbation to the initial values of the trajectory and simulating the resulting behavior of the system checking if it stumbles or if it returns to the periodic motion. If these perturbations are not consistent with the initial phase-separating manifold, it is often customary to apply coupled consistent perturbations instead, like in the case of the hopper to y_b and ϕ_l (compare eqn. (13), and note the brace in the table below). The robot can recover from the following maximum perturbations of its initial values under the invariant influence of its periodic actuations given in figure 6:

ϕ_b	$+133\%$	-63%	$\dot{x}_b$	$+39\%$	-90%
y_b }	-3%	$+0.6\%$	$\dot{y}_b$	$+5000\%$	-100%
ϕ_l }	$+57\%$	-17%	$\dot{\phi}_b$	$+23\%$	-42%
			$\dot{\phi}_l$	$+27\%$	-46%.

For the non-periodic variable x_b of course arbitrary initial values can be chosen. Figure 7 illustrates the differences between the original periodic trajectory and one for which the initial value of $\dot{x}_b$ has been perturbed by -90%. Obviously the robot stays synchronized with its exciting frequency. The perturbed trajectory is characterized by shorter steplengths,

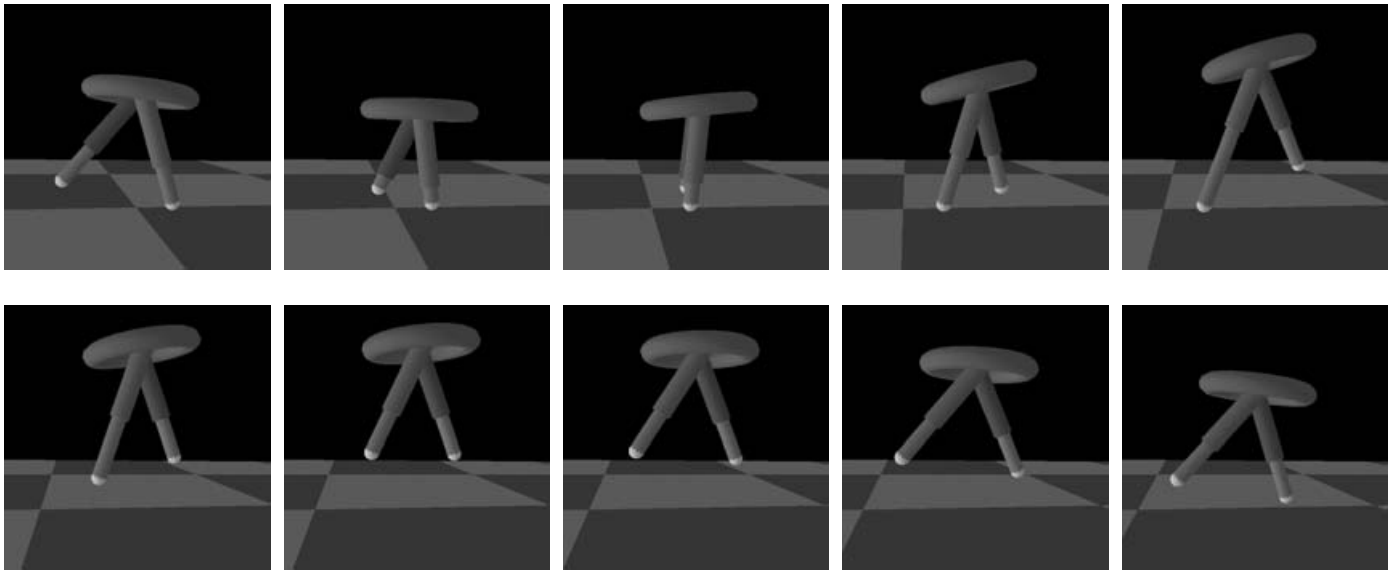

Fig. 9. Most stable open-loop running motion.

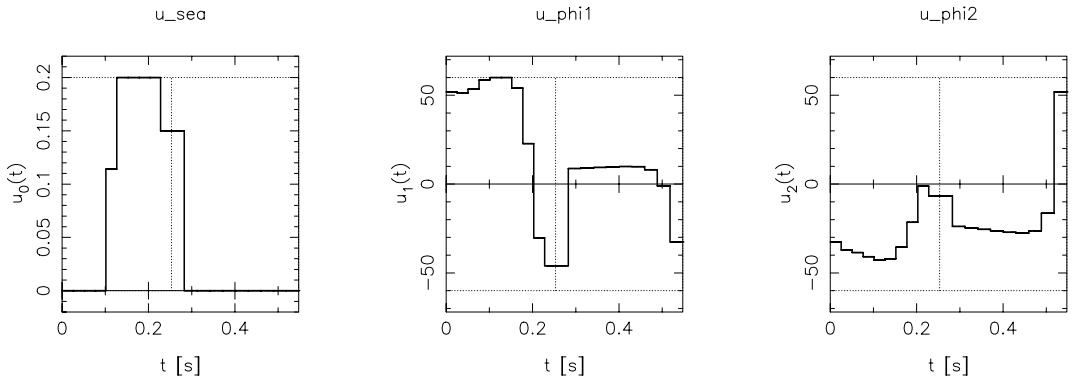

Fig. 10. Actuator patterns for most stable solution of running biped.

https://doi.org/10.1017/S026357470400058X Published online by Cambridge University Press

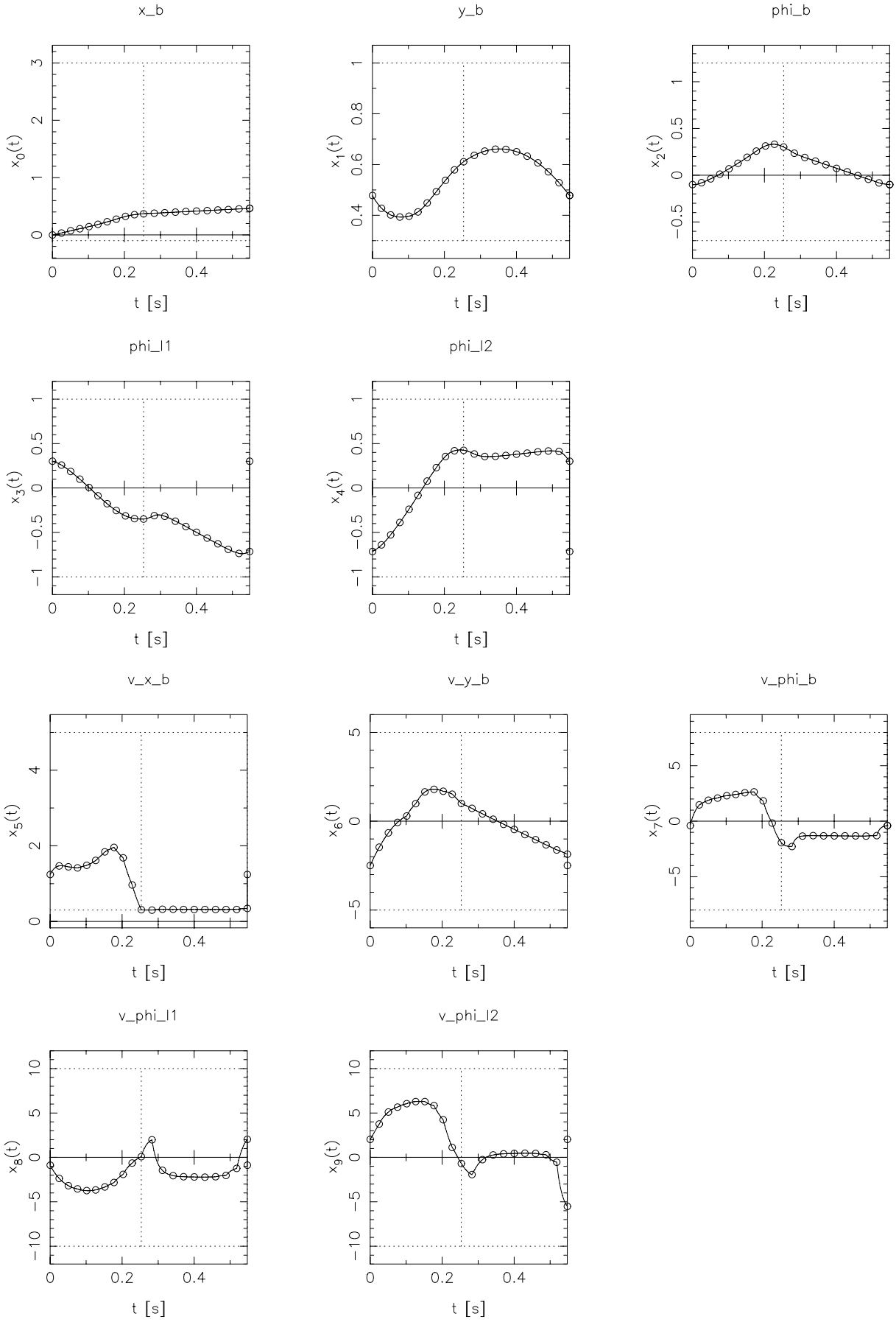

Fig. 11. Position and velocity trajectories of most stable solution of running biped robot.

https://doi.org/10.1017/S026357470400058X Published online by Cambridge University Press

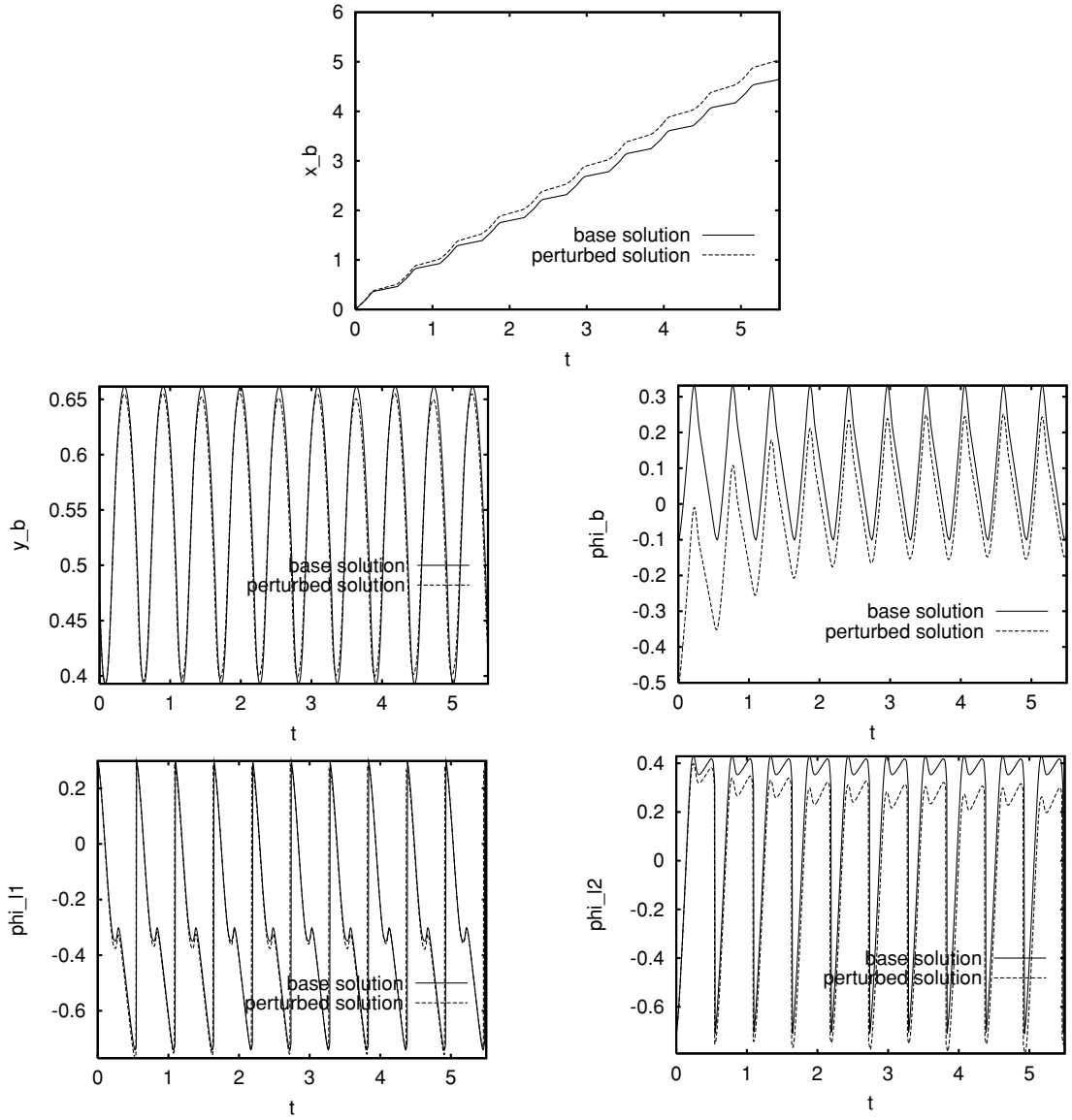

Fig. 12. Effect of perturbation (of ϕ_b by +400%) on most stable trajectory of running robot.

i.e. it stays behind the base solution in the non-periodic variable x_b, as shown in figure 8.

For manufacturing a robot according to these numerical results, it is also interesting to know in which range of model parameter values the robot would persist in its hopping motion:

Θ_b	+5%	−1%	$\Delta\phi$	+96%	−45%
m_l	+5%	−20%	b_{tors}	+1%	−5%
Θ_l	+4%	−23%	k	+1%	−0.4%
d	+11%	−37%	b	+0.5%	−2%.
k_{tors}	+3%	−9%			

5. MOST STABLE SOLUTION OF THE TWO-LEGGED RUNNING ROBOT

The most stable solution found for the two-legged running robot has a spectral radius of 0.8168. Figure 9 shows one model cycle (i.e. one step) of this solution. The model parameter values of the solution are $m_b = 2.0$, $\Theta_b = 0.3465$, $m_l = 0.2622$, $\Theta_l = 0.182$, $d = 0.11$, $l_0 = 0.5$, $k_{tors} = 11.08$, $\Delta\phi_l = 0.5$, $b_{tors} = 9.989$, $k = 606.8$, and $b = 42.48$.

The corresponding cycle time is $T = 0.5476$ s for one step with $T_{contact} = 0.2533$ s and $T_{flight} = 0.2943$ s and the initial values

$$x_0^T = (0.0, 0.4777, -0.1, 0.3, -0.7, 1.240, -2.490, -0.3941, -0.8908, 2.032)$$

Its step length is 0.4637 m.

The full trajectories for all position and velocity variables are given in figure 11 while the corresponding actuator inputs are given in figure 10. Note the u_{SEA2} is identically zero during the step in which leg No. 2 has no ground contact and is therefore not visualized.

https://doi.org/10.1017/S026357470400058X Published online by Cambridge University Press

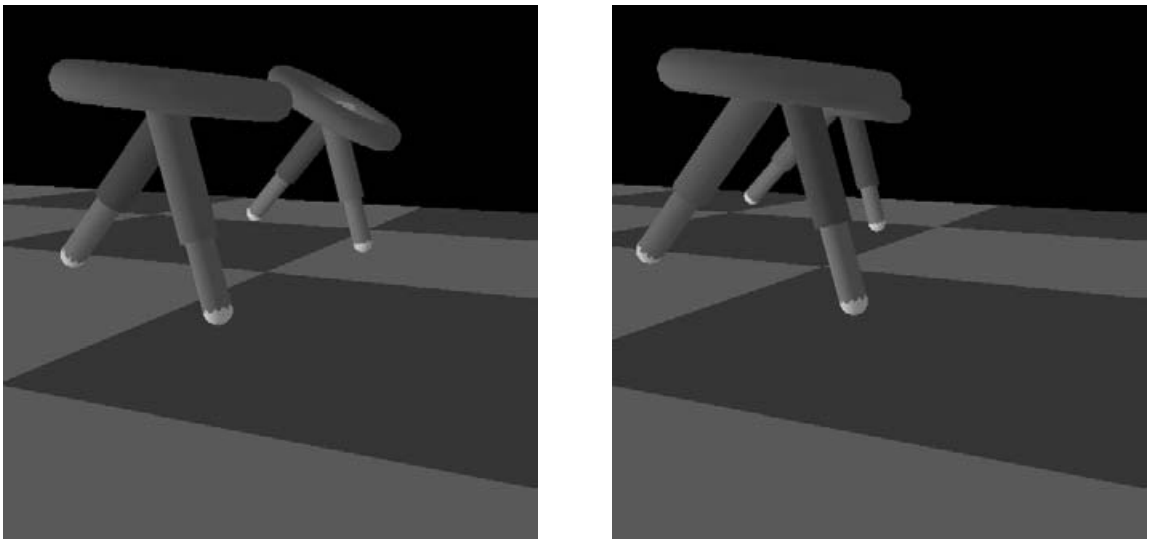

Fig. 13. Comparison of perturbed (back) and unperturbed robot (front) at the start point (left picture) and after nine steps (right picture).

The related monodromy matrix has the following eigenvalues by magnitude:

$$|\lambda_1| = 0.6228 \qquad |\lambda_6| = 0.0515$$
$$|\lambda_{2,3}| = 0.8168 \qquad |\lambda_7| = 0.0001$$
$$|\lambda_4| = 0.8168 \qquad |\lambda_{8,9}| = 0.0$$
$$|\lambda_5| = 0.5373$$

In the optimum, one real eigenvalue and a conjugate complex couple have the same maximum value.

The region of stability in which the robot can recover and maintain a gait without falling down is described by the stability margins

ϕ_b	+400%	−3%	$\dot{x}_b$	+1%	−0.1%
y_b	−0.046%	+0.0.5%	$\dot{y}_b$	+3%	−0.5%
ϕ_{l_1}	+0.184%	−2%	$\dot{\phi}_b$	+12%	−1%
ϕ_{l_2}	+3%	−0.1%	$\dot{\phi}_{l_1}$	+7%	−0.1%.
			$\dot{\phi}_{l_2}$	+0.2%	−5%.

As in the case of the monopod, arbitrary start values are obviously possible for the non-periodic variable x_b. In figure 12 we compare the trajectory starting from a perturbed value of ϕ_b (+400%) with the corresponding unperturbed solution.

For the same perturbation, figure 13 visualizes the positions of unperturbed and perturbed robots at the start point and after nine steps. The left picture clearly shows the large initial perturbation of ϕ_b. In the right picture, this perturbation is nearly damped out, but the slower forward propagation induced by this perturbation is clearly visible (also see first and third plots in figure 12).

The following table finally lists the maximum possible perturbations of model parameters:

Θ_b	+0.5%	−5%			
m_l	+1%	−0.1%	$\Delta\phi$	+100%	−1%
Θ_l	+0.1%	−0.5%	b_{tors}	+0.2%	−0.05%
d	+1%	−5%	k	+0.05%	−2%
k_{tors}	+1%	−0.1%	b	+0.02%	−0.3%

6. CONCLUSIONS

We have presented monopods and bipeds that are capable of stable running motions involving flight phases while not relying on any feedback. Since these robots only have point feet, we have demonstrated that a large foot curvature (and a low center of mass) are not necessary for stability. Self-stabilizing motions are possible even though there are no statically stable standing positions. Furthermore, we have presented recently developed numerical optimization methods for the computation of such open-loop stable robots.

Acknowledgments

The first author would like to acknowledge financial support by the German Research Council (DFG) within the *International Graduiertenkolleg "Complex Processes: Modeling, Simulation and Optimization"*, University of Heidelberg.

References

1. M. H. Raibert and I. E. Sutherland, "Machines that walk," *Scientific American* **248**(1), 32–41 (Jan. 1983).
2. H. de Man, D. Lefeber and J. Vermeulen, "Design and control of a one-legged robot hopping in irregular terrain," *Biology and Technology of Walking*, pages 173–180, Euromech Colloquium 375, Munich (1998) pp. 173–180.
3. J. Vermeulen, D. Lefeber and B. Verrelst, "Control of foot placement, forward velocity and body orientation of a one-legged hopping robot," *Robotica* **21**(1), 45–57 (2003).
4. MIT Leg Lab, "Leg lab robots," http://www.ai.mit.edu/projects/leglab/robots/robots-main.html, 2003.
5. C. M. Thompson and M. H. Raibert, "Passive dynamic running," **In**: (V. Hayward and O. Khatib, editors) *Proceedings of International Symposium of Experimental Robotics* (Springer-Verlag, New York, 1989) pp. 74–83.
6. T. McGeer, "Passive bipedal running," *Proceedings of the Royal Society of London* **B 240**, 107–134 (1990).
7. R. P. Ringrose, "Self-stabilizing running," *Technical Report* (Massachusetts Institute of Technology 1997).
8. T. E. Wei, G. M. Nelson, R. D. Quinn, H. Verma and S. L. Garverick, "Design of a 5-cm monopod hopping robot," *Proceedings of IEEE International Conference on Robotics and Automation*, (2000) pp. 2823–2828. http://www.fluggart.cwru.edu/icra2000/icra2000.html.

https://doi.org/10.1017/S026357470400058X Published online by Cambridge University Press

9. J. G. Cham, S. A. Bailey, J. E. Clark, R. J. Full and M. R. Cutkosky, "Fast and robust: Hexapedal robots via shape deposition manufacturing," *Int. J. Robotics Research* **21**, 10–11 (2002).
10. M. Buehler, "Dynamic locomotion with one, four and six-legged robots," *Journal of the Robotics Society of Japan* **20**(3), 15–20 (April, 2002).
11. T. McGeer, "Passive dynamic walking," *Int. J. Robotics Research* **9**, 62–82 (1990).
12. M. J. Coleman, "A stability study of a three-dimensional passive-dynamic model of human gait," *PhD thesis* (Cornell University, February 1998).
13. M.-Y. Cheng and C.-S. Lin, "Measurement of robustness for biped locomotion using a linearized Poincaré map," *Robotica* **14** Part 2, 253–259 (1996).
14. Y. Hurmuzlu, "Dynamics of bipedal gait: Part II – Stability analysis of a planar five-link biped," *Journal of Applied Mechanics* **60**, 337–343 (June, 1993).
15. K. D. Mombaur, H. G. Bock, J. P. Schlöder and R. W. Longman, "Human-like actuated walking that is asymptotically stable without feedback," *Proceedings of IEEE International Conference on Robotics and Automation*, Seoul, Korea (May, 2001) pp. 4128–4133.
16. K. D. Mombaur, "Stability Optimization of Open-loop Controlled Walking Robots," *PhD thesis* (University of Heidelberg, 2001). www.ub.uni-heidelberg.de/archiv/1796. VDI-Fortschrittbericht, Reihe 8, No. 922, ISBN 3-18-392208-8.
17. G. A. Pratt and M. M. Williamson, "Series Elastic Actuators," *Proceedings of IROS*, Pittsburgh (1995) pp. 399–406.
18. K. D. Mombaur, H. G. Bock, J. P. Schlöder and R. W. Longman, "Open-loop stable solution of periodic optimal control problems in robotics," (submitted to *Zeitschrift für Angewandte Mathematik und Mechanik* (ZAMM, 2003)).
19. E. Garcia, J. Estremera and P. Gonzales de Santos, "A comparative study of stability margins for walking machines," *Robotica* **20**, 595–606 (2002).
20. M. Vukobratovic, B. Borovac, D. Surla and D. Stokic, *Scientific Fundamentals of Robotics 7: Biped Locomotion – Dynamics, Stability, Control and Applications* (Springer, 1990).
21. J. Grizzle, G. Abba and F. Plestan, "Asymptotically stable walking for biped robots: Analysis via systems with impulse effects," *IEEE Transactions on Automatic Control* **46**(1), 51–64 (2001).
22. H. G. Bock and K.-J. Plitt, "A multiple shooting algorithm for direct solution of optimal control problems," *Proceedings of the 9th IFAC World Congress, Budapest*. International Federation of Automatic Control (1984) pp. 242–247.
23. D. B. Leineweber, "Efficient Reduced SQP Methods for the Optimization of Chemical Processes Described by Large Sparse DAE Models," *PhD thesis* (University of Heidelberg, 1999). VDI-Fortschrittbericht, Reihe 3, No. 613.
24. H. G. Bock, "Randwertproblemmethoden zur Parameteridentifizierung in Systemen nichtlinearer Differentialgleichungen," **In**: *Bonner Mathematische Schriften* 183 (Universität Bonn, 1987).
25. M. Winckler, "Numerische Werkzeuge zur Simulation, Visualisierung und Optimierung unstetiger dynamischer Systeme," *PhD thesis* (Universtät Heidelberg, 2000) Cuvillier Verlag, ISBN 3-89873-060-3.

https://doi.org/10.1017/S026357470400058X Published online by Cambridge University Press